ELSEVIER

Thermochimica Acta 304/305 (1997) 239–249

thermochimica acta

Comparison of DSC heating rate and HCS frequency at the glass transition

E. Donth*, J. Korus, E. Hempel, M. Beiner

Universität Halle, Fachbereich Physik, D-06099 Halle (Saale), Germany

Received 27 July 1996; accepted 12 December 1996

Abstract

Heat capacity spectroscopy HCS and differential scanning calorimetry DSC results are compared for eight polymers (especially for polyisobutylene (PIB) and a random copolymer of *n*-butyl methacrylate with 8% styrene) and glycerol. A mean value of the parameter a is obtained as $\bar{a} = 4.3 \pm 2$, where $a \equiv \dot{T}/\delta T \omega_{max}$, with $\dot{T}$ the DSC heating rate, δT the temperature dispersion from the DSC transformation interval, and ω_{max} the frequency of the imaginary part of maximum heat capacity, extrapolated from HCS to DSC temperatures. The results are discussed with regard to the fluctuation dominance of molecular glass transitions, to the fluctuation dissipation theorem, and to the Second Law of Thermodynamics. The a value seems to be universal, not depending on the substance group and fragility. © 1997 Elsevier Science B.V.

Keywords: Differential scanning calorimetry (DSC); Fluctuation dissipation theorem (FDT); Glass transition; Heat capacity spectroscopy (HCS)

1. Introduction

At a given temperature T, the dynamic glass temperature as determined by heat capacity spectroscopy (HCS) [1] is characterized by the frequency ω_{max} (in rad/s) of the $C_p''(\omega)$ peak maximum. $C_p''(\omega, T)$ is the imaginary part of the dynamic or complex heat capacity, usually determined by linear response in equilibrium. As determined by differential scanning calorimetry (DSC) [2], however, the thermal glass temperature is characterized by a temperature program, e.g. by the heating rate $\dot{T}$ (in K/min). This glass temperature can be determined by an equal-area construction from the DSC thermogram for heating, if the heating rate is equal to the preceding cooling rate with no annealing period in-between. The transition from the non-equilibrium glass state to the equilibrium liquid state is influenced by structural relaxation [3].

Fig. 1 compares both methods for glycerol. Irrespective of the experimental differences it seems that, after some horizontal shift to bridge over the gap between HCS and DSC glass temperatures, corresponding pairs $(\omega_{max}, \dot{T})$ can be determined, where the $C_p'(T; \omega_{max})$ curve from HCS coincides [4] with the $C_p(T; \dot{T})$ curve from DSC if the latter is properly corrected $(C_p \rightarrow C_p')$ for structural relaxation. The corresponding relation between $\dot{T}$ and ω_{max} is the subject of this paper.

Since it is difficult to apply HCS at low frequencies [5] (too long temperature wavelengths in the sample) and since DSC results at high $\dot{T}$ values are falsified by serious heat transfer problems, it seems that the HCS–DSC temperature gap of the order of a few 10 K cannot easily be shortened. We are therefore confronted with

*Corresponding author.

PII S0040-6031(97)00027-0

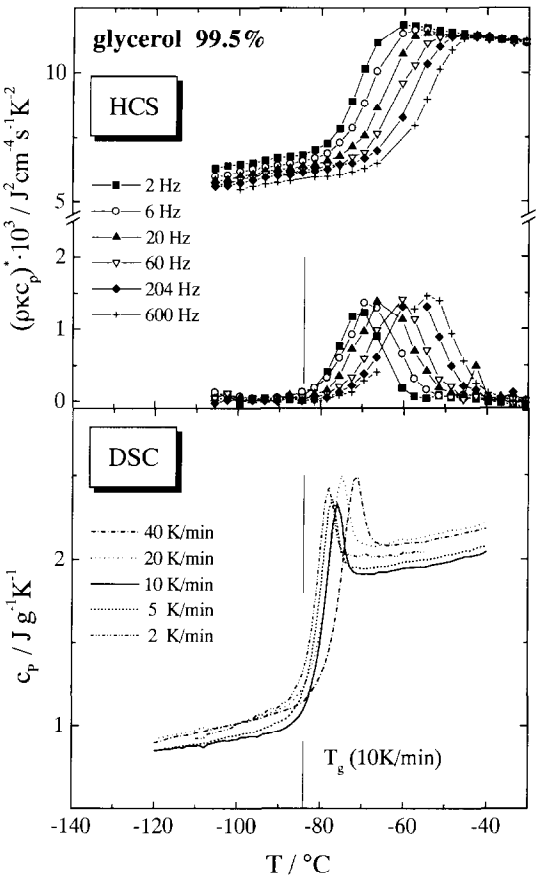

Fig. 1. Dynamic heat capacity results from HCS: Real and imaginary parts of $(\rho\kappa c_p)^*$ as a function of temperature at different constant frequencies $\nu = \omega/2\pi$ (upper part), compared with heat capacity from DSC as a function of temperature at different heating rates $\dot{T}$ after equal cooling rates with no annealing (lower part) for glycerol of 99.5% purity. κ = heat conductivity, ρ =mass density. In all c_p^* figures, the real part is on the top.

non-trivial extrapolation problems to bridge over the gap. A way out seems to be [6] the use of temperature-modulated DSC, TMDSC [7], allowing fairly low frequencies for the $C_p^*(T,\omega)$ determination. Unfortunately, the TMDSC advantages of no temperature gap, and the use of only one single apparatus with the same thermometers for both measurements, are at present partly lost by a seemingly complicated structural-relaxation effects on the low temperature $C_p''(T)$ flank. This will be discussed in a separate paper [8].

Despite the obviously better chances for TMDSC in the future, it seems to be useful to take the many HCS results from our laboratory [9] for a rough determination of the desired $\{\omega_{max}, \dot{T}\}$ relation. The aim of this paper is to compare HCS and DSC for nine glass formers in three-substance groups:

1. 'normal' glass transitions (glycerol, natural rubber (NR), polyvinylacetate (PVAC), and a random copolymer of styrene and butadiene, SBR rubber),
2. 'complex' glass transitions (such as in polyisobutylene (PIB) and bromobutyl rubber (BIIR)), where probably two glass transitions are in the main transition [10], and
3. substances where the glass transition is near the cooperativity onset [11], here called 'near-onset' substances, such as three random copolymers of *n*-butyl methacrylate, P(*n*BMA-stat-S), with 2%, 8% and 19% mol styrene.

In the next section a theoretical background will be described to show that there is an unsolved theoretical problem behind the $\{\dot{T}, \omega_{max}\}$ relation. The ratio [12]

$$a = \dot{T}/\delta T \omega_{max}, \tag{1}$$

where δT is a temperature difference related to the glass-transition interval, will be defined as a basis for the discussion of the experimental results. We find an average value $\log_{10} a = 0.63 \pm 0.2$ confirming Hensel's TMDSC results $a = 6 \pm 1$ for PVAC and a semicrystalline poly(ether etherketone) [6].

2. Theoretical

This section is an attempt to describe the theoretical problem behind the a constant according to Eq. (1). The main idea is to find out how Nature itself makes 'calorimetry', i.e. how much time is needed in the fluctuation formula [13]

$$kC_p = \overline{\Delta S^2} \tag{2}$$

for the time averaging of entropy fluctuation ΔS^2 to establish a heat capacity C_p; and k is the Boltzmann constant.

Let us start with the linear material equation for entropy response,

$$\mathrm{d}S = \int_{-\infty}^{t} \frac{C_p(t-t')}{T} \dot{T}(t')\mathrm{d}t', \tag{3}$$

where $C_p(t-t')/T$ is the entropy compliance and $T(t')$ the temperature program in the past $t' \leq t$, $\dot{T}(t') = \mathrm{d}T/\mathrm{d}t(t')$. Using

$$C_p^*(\omega) \equiv C_p^g + \int_0^\infty \dot{C}_p(\tau)\exp(-\mathrm{i}\omega\tau)\mathrm{d}t = C_p'(\omega) - \mathrm{i}C_p''(\omega), \quad (4)$$

we see that the relation between $\dot{T}$ and ω_{max} is not monitored by a temperature interval as defined in Eq. (1), but by the temperature T itself. Such a reduction will be expressed by a tilde over a:

$$\text{Eq.(3) with } \omega\tau \approx 1 \Rightarrow \tilde{a} \equiv \dot{T}/T\omega_{max} = 0(1). \quad (5)$$

This means that the heating rate should be reduced by the (glass) temperature to get a ratio $\tilde{a}$ of order 1. From experience [6,12], we know that a heating rate of 10 K/min corresponds to a frequency of only a few millihertz, e.g. $\omega_{max} \approx 6$ mrad/s. This would imply an $\tilde{a}$ value of ~ 0.1 for $T \equiv T_g = 300$ K, obviously too small for the Eq. (5) estimation of the simple linear response Eq. (3).

Let us now analyze our 'a' problem with the aid of the fluctuation dissipation theorem FDT. We start from the enthalpic First Law fundamental form (i.e. from enthalpy H),

$$\mathrm{d}H = T\mathrm{d}S + V\mathrm{d}p. \quad (6)$$

Considering an isobaric temperature disturbance, the FDT [14] in the frequency domain reads

$$\Delta S^2(\omega) = kTJ_S''(\omega)/\pi\omega. \quad (7a)$$

This equation can be interpreted as an equation for a natural experiment: it connects the linear response of the system (dynamic entropy compliance $J_S^* = J_S' - \mathrm{i}J_S''$), caused by an external disturbance, with internal thermal fluctuations (entropy spectral density $\Delta S^2(\omega)$) of the subsystem considered. In the linear regime the $\Delta S^2(\omega)$ function does not depend on the external disturbance, i.e. we have the same $\Delta S^2(\omega)$ function also in case of no disturbance. Using

$$C_p^*(\omega) = TJ_S^*(\omega) \quad (7b)$$

and the sum formula

$$\overline{\Delta S^2} = \int_{-\infty}^{\infty} \Delta S^2(\omega)d\omega \quad (8)$$

we get

$$\overline{\Delta S^2} = (2k/\pi)\int_{\omega=0}^{\infty} C_p''(\omega)\mathrm{d}\ln\omega = kC_p. \quad (9a)$$

Integration over the glass transition C_p'' peak only would give

$$\overline{\Delta S^2} = k\Delta C_p. \quad (9b)$$

The π^{-1} factor in Eq. (9a) comes from the definition used for the Fourier transformation between spectral density $y^2(\omega)$ and correlation function $y^2(\tau)$,

$$y^2(\omega) = \pi^{-1}\int_0^\infty \mathrm{d}\tau\cos(\omega\tau)y^2(\tau), \quad (10)$$

or, in other words, from the Kramers–Kronig dispersion relations of any variable y.

In this picture, the thermal glass transition for a cooling experiment is schematically shown in Fig. 2. Cooling shifts the glass-transition $C_p''(\omega)$ peak to a lower frequency, and, somewhat simplified, at a certain frequency ω_{max}, defined by the a and δT values of Eq. (1), the time in the time averages of Eqs. (2),(9a) and (9b) becomes too short for contributing to the experimental C_p value: We observe the well-known C_p step at T_g, ΔC_p, because the hatched part in $C_p''(\log\omega)$ is cancelled in Eq. (9b) by the freezing-in.

A relation between $\dot{T}$ and ω_{max} needs the reduction of $\dot{T}$ by a temperature or a temperature interval, named δT in Eq. (1). The description by the FDT suggests the use of temperature *fluctuation* for δT. As is well

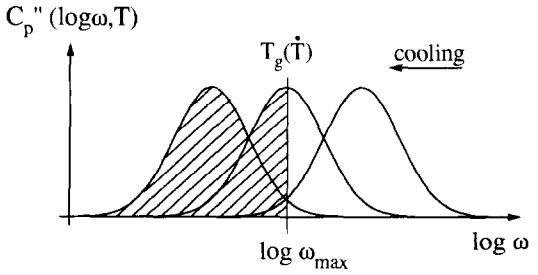

Fig. 2. Thermal glass transition for cooling, schematically presented as freezing-in of dynamic heat capacity below a frequency ω_{max} corresponding to a cooling rate $\dot{T}$ according to Eq. (1). The hatched areas can no longer contribute to C_p. Structural relaxation is neglected.

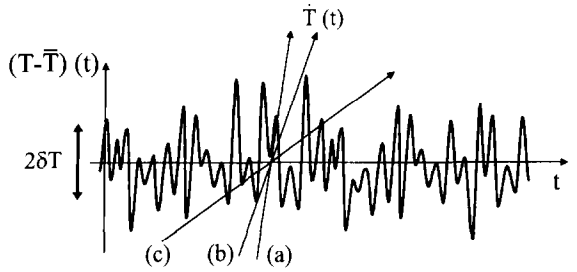

Fig. 3. Temperature fluctuation of a cooperativity region as a function of time t, compared with three examples for heating rate $\dot{T}(t)$. For details see text. Case (b) is assumed to correspond to Eq. (1).

known, the relative temperature fluctuation of millimeter samples is of the order of 10^{-10} K or smaller, beyond the scope of any discussion with Eq. (1). The main idea [12,14] is to use a small subsystem for getting a larger δT; more precisely, to use the cooperativity region [15] of size 2...3 nm [16] as the representative subsystem for the description of dynamic glass transition, and the requirement that the microscopic description of the dynamics be dominated by such fluctuations [17].

The temperature fluctuation of the cooperativity region is depicted in Fig. 3. The dispersion of this subsystem fluctuation is denoted by δT. The a problem is now a comparison of a heating (or cooling) rate with the fluctuation rate. Three abstract variants are shown: (a) The rate $\dot{T}$ is too large, i.e. the time is too short for detecting the fluctuation; (b) is the transition case for Eq. (1); and (c) a variant in which there is no problem for time averaging in Eqs. (9a) and (9b) because of a sufficiently slow rate. Dominance of fluctuation gives the relation between the experimental time τ_{exp} for establishing the time average in Eq. (9b) (case (b)) to the fluctuation interval δT,

$$\tau_{exp} = \delta T/\dot{T}. \tag{11}$$

From Eq. (1), we see that the a parameter reads

$$a = 1/(\tau_{exp} \cdot \omega_{max}). \tag{12}$$

The a parameter thus corresponds to a rate: How fast can a fluctuating oscillation (ω_{max}) be realized (thermodynamically be measured) by a drift $\dot{T}$ in the fluctuation dispersion interval δT. This interpretation suggests a universal value for a.

As far as we know there is as yet no theoretical approach on how this ratio can be calculated. As already mentioned, $a \approx 6$ or somewhat smaller, but of order one.

It should be mentioned that the Narayanaswamy–Moynihan–Hodge formulas for structural relaxation [18] are also burdened with this real time problem. It is well known that these formulas contain four adjustable parameters,

$$\{\tau_g,\ B,\ x,\ \beta\} \tag{13}$$

where, in modern terms, B stands for fragility, x for non-linearity, β for non-exponentiality, and τ_g for a 'glass time'. The determination of τ_g is connected to the a value of Eq. (1). Practically, it is solved by a horizontal shift of the calculated to the measured $C_p(T)$ curves.

3. Experimental

The heat capacity spectrometer (also HCS) was built in our laboratory [9,19,20]. It is an improved version, as compared to Nagel's 3ω spectrometer [1], with regard to temperature stability, clamping of polymer samples, and electronic signal detection. Polymers with rather small $\Delta c_p/\overline{c_p}$ values of several percent can now be analyzed. The details are described in a separate paper of this issue [19]. The δT values are determined as dispersions from a Gauss fit of $C_p''(T)$ curves at constant frequency [12,17].

For the heating or cooling rate experiments, a Perkin–Elmer DSC7 was used, the sample mass being a few milligrams. T_g was determined from an equal-area construction for both heating and cooling thermograms (no annealing in-between). The heat transfer problems were partly eliminated by taking the average between heating and cooling. An exact comparison between HCS and DSC would require the calculation of an equilibrium C_p^* response from the thermograms by using structural relaxation corrections. This was approximated by two steps. First, the δT values were estimated from

$$\delta T = \Delta T_h/2.5 \quad \text{from heating} \tag{14a}$$

$$\delta T = \Delta T_c/4.0 \quad \text{from cooling,} \tag{14b}$$

where ΔT is the temperature interval between 16% and 84% of the total ΔC_p step. The numbers 2.5 and 4.0 were estimated from the more precise analysis of Ref. [21]. Second, it was assumed that the $C_p''(\omega)$

maximum corresponds to the equal area T_g, i.e. that the $C_p''(\log\omega)$ peak is symmetrical. The log symbol in this paper always means $\log_{10}$.

The uncertainties of a values, obtained from Eq. (1), determined by this HCS-DSC comparison are considerable. The main sources are

1. Mutual uncertainty of the sample temperature scale in the two different devices (up to 0.6 K).
2. Uncertainty of δT values (up to 20% for HCS, up to 50% for DSC).
3. Uncertainty from WLF extrapolation (see Fig. 9, later) for bridging over the gap between DSC and HCS temperatures (strongly depending on the substances, ranging from ± 0.3 to ± 1.2 for log a).
4. Uncertainty of the $T_g - \omega_{max}$ equivalence.
5. Uncertainty of the a fitting by mutual shifting of the $\log\dot{T}$ scale for DSC against the $\log\omega_{max}$ scale for HCS curves (up to 50%).

The total log a uncertainty was estimated individually for each substance: it was ranged between $\Delta\log a = \pm 0.5 \ldots \pm 1.5$. This means that the uncertainty of an individual a value is at least a factor of three.

The WLF extrapolation was either based on the curvature of the HCS trace in an Arrhenius diagram ($\log\omega_{max}$ vs. $1/T$), or on parallel dielectric experiments adapted [20] to the HCS values.

4. Results

Fig. 4 shows the HCS $C_p^*(T,\omega)$ values as a function of $\log\omega$ for glycerol (group (i) substance). The temperature curves were compared to the DSC $C_p(T,\dot{T})$ function in Fig. 1. The $C_p''(\log\omega)$ curves are rather symmetrical, and the extrapolation gap between DSC and HCS temperatures is ca. 15 K. The HCS $C_p^*(T,\omega)$ functions for the group (ii) substance PIB are shown in Fig. 5. The corresponding T curves are compared to the DSC results in Fig. 6. The $C_p''(\log\omega)$ curves for PIB are not symmetrical, they indicate a smaller slope of the *low* frequency flank which is not often observed in glass formers. The extrapolation gap is ca. 20 K. The HCS $C_p^*(T,\omega)$ results for the group (iii) (near-onset) substance P(*n*BMA-stat-S) with 8% mol S are presented in Fig. 7, their comparison with DSC ther-

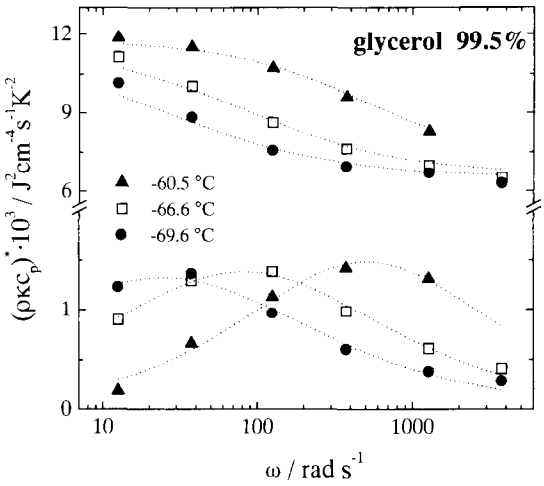

Fig. 4. HCS results for glycerol 99.5% as a function of log frequency for several temperatures. The dotted lines are symmetrical Havriliak–Negami fits [25].

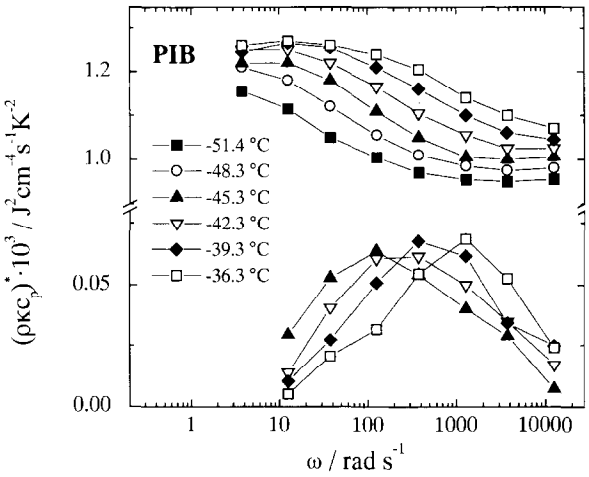

Fig. 5. HCS results for polyisobutylene (PIB) as a function of log frequency for different temperatures. Observe the asymmetry of the imaginary part.

mograms is in Fig. 8. $C_p''(\log\omega)$ seems to be symmetrical, and the extrapolation gap is ca. 20 K.

The comparison method for the $\dot{T}/\omega_{max}$ relation, i.e. the $\log\dot{T} - \log\omega_{max}$ relation, is schematically illustrated in Fig. 9. The first step is to get a WLF curve from either dielectric experiments adapted to HCS (glycerol) or from HCS itself (PIB, copolymer). This curve is drawn into an Arrhenius diagram $\log\omega$ vs

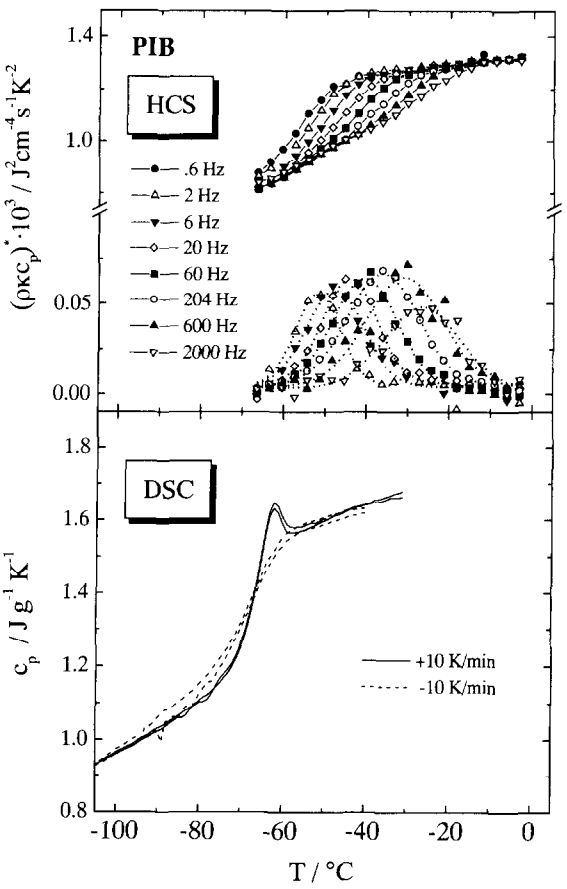

Fig. 6. HCS results for PIB as a function of temperature for different frequencies (upper part) as compared with two DSC cooling–heating runs at 10 K/min (lower part). The fits of the imaginary part are Gaussian functions for determining the dispersion δT.

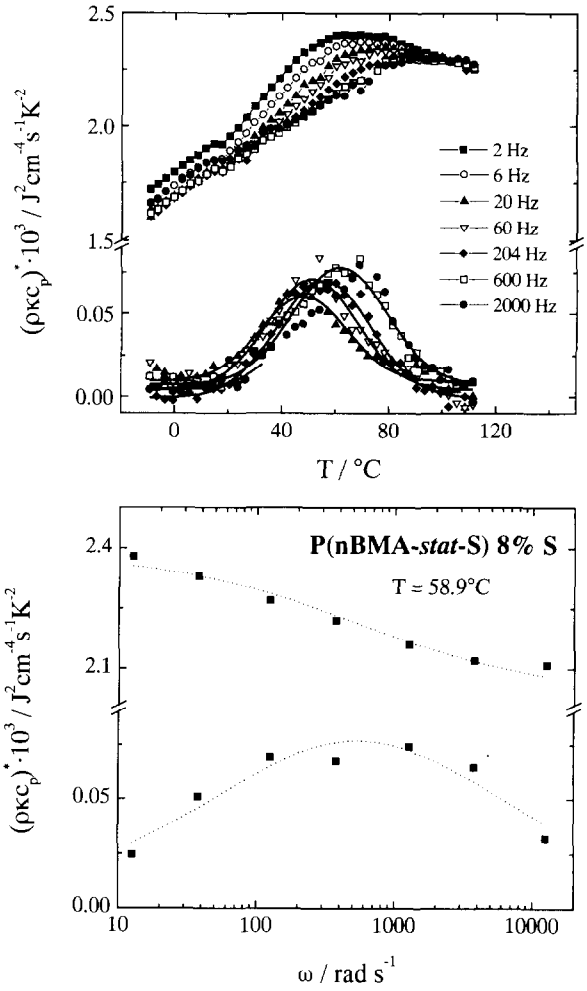

Fig. 7. HCS results for the random copolymer P(nBMA-stat-S) with 8% mole S (nBMA = n – butyl methacrylate, S = styrene). Upper part: as a function of temperature. Lower part: as a function of frequency. The lower part curves are symmetrical Havriliak–Negami fits.

$1/T$. Then the DSC $\log\dot{T}$ vs. $1/T_g$ data are put in the same plot. The $\log\dot{T}$ axis is vertically shifted as long as the DSC data set it best fitted to the HCS original WLF curve. The ordinate difference $\log\dot{T} - \log\omega_{max}$ then gives the $\dot{T}/\omega_{max}$ ratio. The results of this procedure are presented in the upper parts of Figs. 10–12. The lower parts show, as a control, how the δT values from HCS suit to the smaller δT values from DSC.

The $\dot{T}/\omega_{max}$ uncertainty is particularly large in the near-onset group (iii) substance, because of two reasons: The accessible equilibrium glass-transition trace in the Arrhenius diagram is short, and in the so-called $\alpha\beta$ splitting region [11] the ε'' and c_p'' maximum traces depend on the evaluation method: We obtain different traces for isothermal and isochronal maxima. Unfortunately, the HCS frequency window is too small to get many reliable c_p'' isotherms.

The results for all the nine substances investigated are listed in Table 1.

5. Discussion

The Table 1 $\log a$ values, according to Eq. (1) (with δT from DSC, of course), and the $\log\tilde{a}$, values accord-

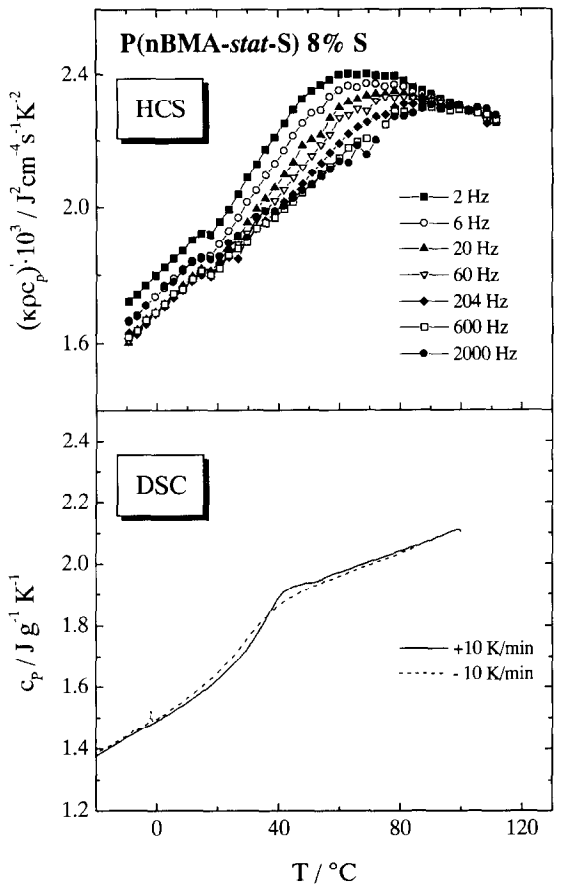

Fig. 8. Real part of HCS results for the 8% copolymer (same data as in Fig. 7, upper part), now as compared with a DSC cooling–heating run.

ing to Eq. (5), are presented in Fig. 13. Selecting the isochronal HCS δT_{20} values for $\nu = 20$ Hz as the abscissa, the substances are assorted into the groups (i) = normal, (ii) = complex, and (iii) = near co-operativity-onset glass transitions. The average log a and log $\tilde{a}$ values are calculated with regard to the individual uncertainties:

$$\overline{\log a} = 0.63 \pm 0.5, \tag{15}$$

and

$$\overline{\log \tilde{a}} = -1.4 \pm 0.5, \tag{16}$$

where the uncertainty is for the individual values (factor 3 for a). The uncertainty of the averages is estimated as about ±0.2, this means a factor of 1.6.

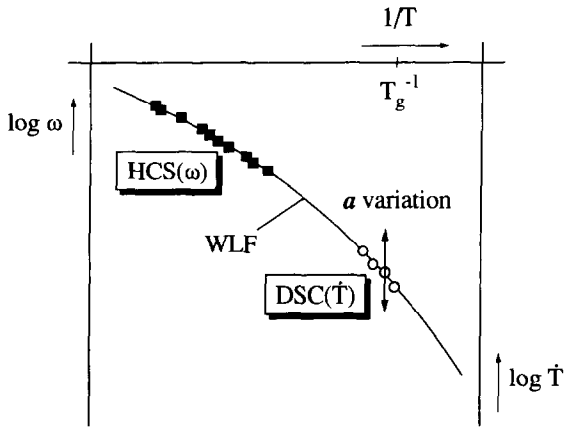

Fig. 9. Schematic diagram for determination of the a parameter in Eq. (1) by vertical variation of DSC results (shifting of log $\dot{T}$). The WLF curve is from HCS (or dielectric experiments adapted to HCS), and the Eq. (1) comparison is made for DSC at $\dot{T} = 10$ K/min and the corresponding DSC δT value.

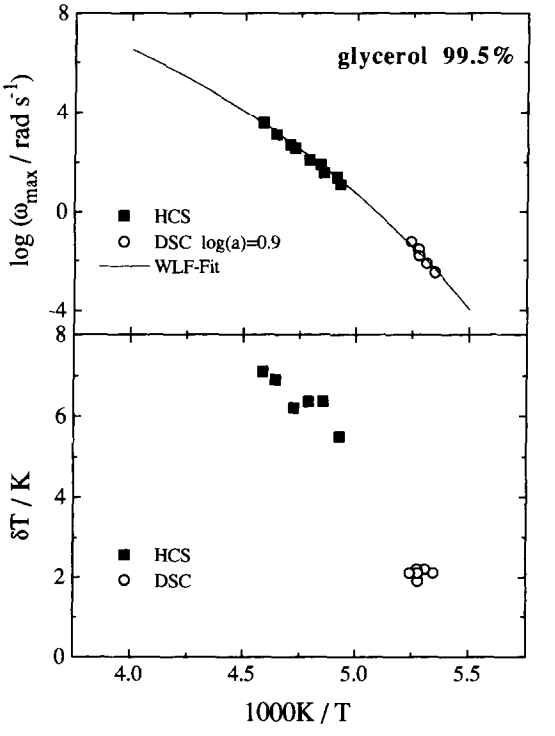

Fig. 10. Actual fit of DSC to HCS for the a determination in 99.5% glycerol. Upper part: Arrhenius diagram. Lower part: Temperature dispersion δT from HCS and DSC as a function of temperature. The consistency of both δT series is satisfactory.

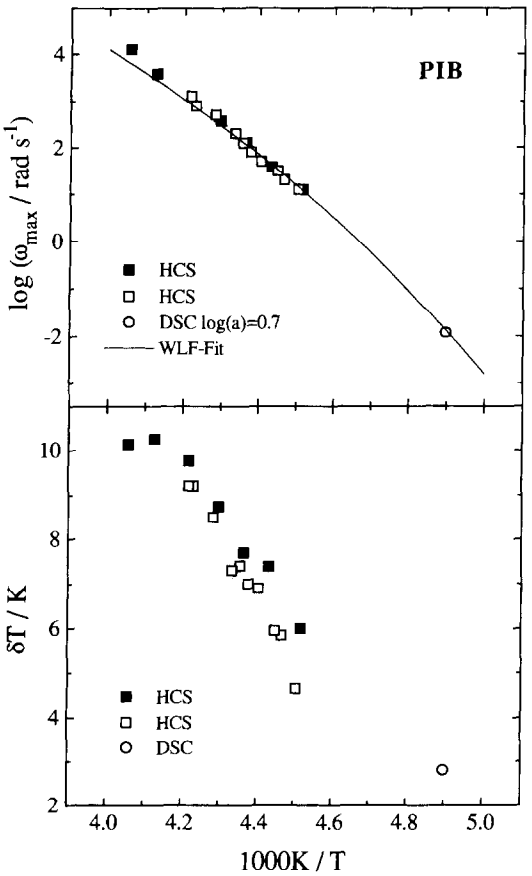

Fig. 11. Determination of a for PIB (details see Fig. 10). The (■) and (□) symbols are from two independent HCS experiments.

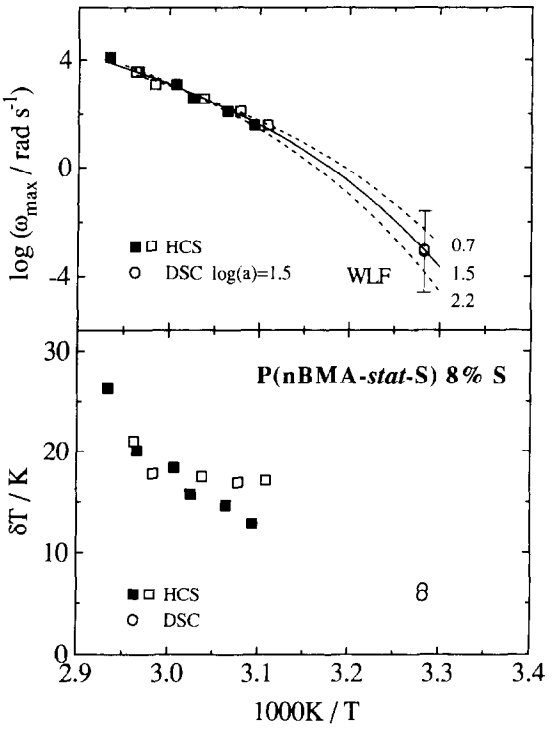

Fig. 12. Determination of a for the 8% copolymer (for details see Fig. 10). The (■) and (□) symbols are from two independent HCS experiments. The middle WLF fit is from points of both HCS experiments with T_∞ from dielectrics (see footnote (b) below Table 1), the broken lines are the WLF fits for each data set, separately. The numbers are the different log a values obtained. The error bar indicates the large total uncertainty of the construction for the near-onset substances.

Therefore, using Eq. (12), we obtained an average value

$$\bar{a} = 4.3 \pm 2 \equiv 1/(\bar{\tau}_{exp}\omega_{max}). \quad (17)$$

This value is consistent with the Hensel $a = 6 \pm 1$ value in the frame of uncertainties. The $\bar{a}$ value obtained is of order one, whereas the average $\bar{\bar{a}}$ value is ~0.04, much smaller than one. This favors the reduction of $\dot{T}$ by δT, and does not favor the reduction by T_g.

Nevertheless, the $\bar{a}$ value obtained corresponds to a relatively short experimental time τ_{exp} when compared to ω_{max}^{-1}, and $\tau_{exp} \approx \omega_{max}^{-1}/4$. Compared to the time for one period, $\tau_p \equiv 1/\nu_{max} = 2\pi/\omega_{max}$, we have

$$\bar{\tau}_{exp}/\tau_p \approx 1/(2\pi\bar{a}) \approx 0.04. \quad (18)$$

This means that the time needed for establishing a heat capacity from entropy fluctuations is only 4% of a mean fluctuation period in case of glass transitions. The reduction with T_g would give a value $1/(2\pi\bar{\bar{a}}) \approx 4$, i.e. four periods would be needed for the establishment. This seems too large.

The obtained a ratios seem to be universal, not depending on the substance group and fragility F (Table 1).

Let us close the discussion with a few general remarks about the relationship between dynamic heat capacity C_p^* and the Second Law. First, let us define $C_p = \dot{Q}/\dot{T}$, with $\dot{Q}$ the heat input per time to the system, and $S = \int C_p d\ln T$ with this C_p, then the HCS of the stationary case corresponds to a thermodynamic cycle. This cycle is irreversible if $\oint dS > 0$.

Table 1

Parameters for 9 glass formers. T_g = glass temperature at 10 K/min from DSC. δT = temperature dispersion from DSC (10 K/min) or HCS (20 Hz). $\delta_{20}\log\omega$ = dispersion of the $C_p''(\log\omega)$ curve at T_{20} from HCS. [$\delta\log\omega = 0.49$ for a Debye relaxation adapted to a $\log\omega$ Gaussian function at the half width, log = $\log_{10}$]. T_∞ and $\log\Omega$ are the asymptotic parameters of the WLF equation: $(T - T_\infty)\log(\Omega/\omega) = (T_0 - T_\infty)\log(\Omega/\omega_0) = \text{const.}$ $F = T_g/(T_g - T_\infty)$ fragility parameter, $a = \dot{T}/\delta T\omega_{max}$ for $\dot{T} = 10$ K/min, Δa = uncertainty of a. The last column indicates whether the WLF equation is from HCS or dielectrics (ε)

Substance	T_g/°C	δT/K	δT_{20}/K	$\delta_{20}\log\omega$	T_{20}/°C	T_∞/°C	$\lg\Omega$	F	$\log a$	$\Delta\log a$	
	10 K/min	DSC	HCS	HCS	HCS		(rad/s)				
Glycerol	−84	1.9	5	0.83	−64	−145	15.6	3.1	0.9	0.6	ε[a]
NR	−68	1.6	5.3	1.12	−55	−98	11.4	6.7	0.3	0.5	ε
PVAC	39	2.4	6.2	1.00	57	−7	12.5	6.7	0.75	0.5	ε
SBR	−55	2.7	6.3	1.15	−39	−84	10.6	7.4	1.0	0.5	HCS
PIB	−69	2.8	8.5	1.07	−46	−142	13.7	2.8	0.7	0.7	HCS
BIIR	−67	2.3	9	1.12	−45	−142	14	2.7	0.0	0.6	ε
2%S copolymer	30	7.5	20.2	–[c]	50	−7	9.5[b]	7.2	0.2	1.3	HCS[b]
8%S copolymer	31	5.7	14.5	–[c]	52	−9	10.7[b]	7.3	1.5	1.5	HCS[b]
19%S copolymer	33	5.5	12	–[c]	51	−4	10.4[b]	8.3	0.5	1.2	HCS[b]
General uncertainty	±2	±20%	±20%	±30%	±2 K[d]	±10 K	±1	±1	—	—	—

[a] Thesis: F. Stickel, Universität Mainz, 1995.

[b] From HCS data, but T_∞ from dielectrics. This mixture was used for bridging over the HCS–DSC gap, because HCS leaves the ε trace in the Arrhenius plot near the onset. The $\log\Omega$ values are conditional and differ considerably from the dielectric $\log\Omega$ values.

[c] Too few data for a reasonable estimation.

[d] ±4 K for the copolymers.

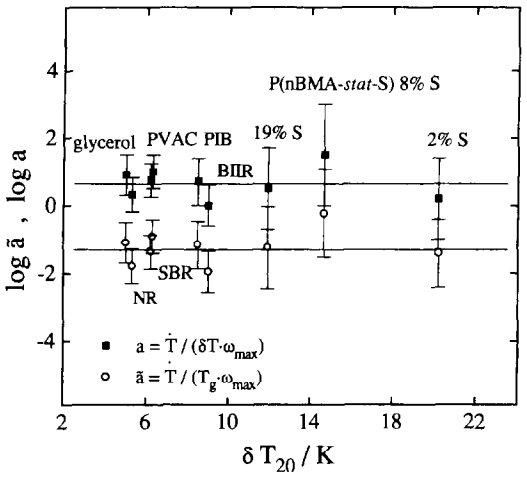

Fig. 13. Values of log a from Eq. (1) (■,□) and log $\tilde{a}$ from Eq. (5) (○) for the nine glass formers as a function of the HCS temperature dispersion at 20 Hz, δT_{20}. This parameter assorts the three substance groups: normal (glycerol, PVAC, SBR, NR), complex (PIB, BIIR), and near-onset (2%S, 8%S, 19%S copolymer). The average lines are calculated by weighting with the different uncertainties ($\overline{\log a} = 0.63$).

From linear response, we get [22]

$$\Delta S_{\text{irrev}} \equiv \oint \mathrm{d}S = \pi(\Delta T)^2 C_p''(\omega, T)/T^2 \geq 0 \text{ for } C_p'' \geq 0, \tag{19}$$

where ΔT is the temperature amplitude of the periodic $T(t)$ program. The $C_p'' \geq 0$ relation thus follows from the Second Law, although there is no 'loss' or 'dissipation' connected with a bare heat input. The mean entropy production is obtained from Eq. (19),

$$\dot{S}_{\text{irrev}} = \omega(\Delta T)^2 C_p''/2T^2. \tag{20}$$

Second, a DSC cooling–heating cycle also corresponds to a thermodynamic cycle. In equilibrium, far from the glass-transition zone ($C_p'' \equiv 0$), we get $\Delta S_{\text{irrev}} = 0$, but including the thermal glass transition we obtain [23]

$$\oint C_p dT = 0 \quad \text{(First Law)}, \tag{21}$$

and

$$\Delta S_{\text{irrev}} = \oint \frac{C_p}{T}\mathrm{d}T > 0 \quad \text{(Second Law)}. \tag{22}$$

An order-of-magnitude estimation gives

$$\Delta S_{\text{irrev}} \approx \Delta C_p \delta T^2/T_g^2 \tag{23}$$

with ΔC_p the C_p step height and δT the half transformation interval at T_g, about corresponding to the temperature fluctuation of the relevant subsystem. Third, using the FDT, Eqs. (7a) and (7b), i.e.

$$\Delta S^2(\omega) = kC_p''(\omega)/\pi\omega, \tag{24}$$

the $C_p''(\omega) \geq 0$ relation can be reasoned seemingly outside (!) the Second Law. As is well known (Ref. [24], Chintchine theorem), $\Delta S^2(\omega) \geq 0$ follows directly from the properties of the correlation function $\Delta S^2(\tau)$, when $\Delta S^2(\omega)$ is defined by the Fourier transformation of a correlation function, Eq. (10), with $y = S$. Hence, $\Delta y^2(\omega) \geq 0$ is a purely mathematical property of *any* spectral density of a stationary stochastic process; here $y = S$ is the entropy fluctuation of the relevant subsystem. One can speculate, in the frame of local equilibrium and linear response, that the Second Law is an implication of the fluctuation dissipation theorem that is here discussed as *the equation* of a natural thermodynamic experiment.

Summarizing the general remarks, $C_p^*(\omega, T)$ is interpreted as dynamic or complex heat capacity of linear response, corresponding to the dynamic entropy compliance, having a real and a positive imaginary (no loss) part, and being a property of a small isobaric thermodynamic TS cycle at a temperature T (pressure p, ...) with a frequency ω.

6. Conclusions

We have demonstrated how the glass-transition frequency $\omega_{\max}$ of a heat-capacity spectroscopy HCS experiment can actually be compared with a heating (or cooling) rate $\dot{T}$ of a DSC experiment for T_g. The uncertainty of the comparison is relatively large, mainly caused by the large gap between the temperatures, where a $C_p''(\omega)$ maximum can be detected in our HCS device and the glass temperatures accessible by standard DSC. It seems that in the future TMDSC would be more appropriate for this issue. The average value obtained for the a ratio, $\bar{a} \equiv \dot{T}/\delta T\omega_{\max} = 4.3 \pm 2$ (relating $\dot{T}$ to the half of the transformation interval δT), is in accordance to the

first TMDSC results obtained by Schick's group in Rostock. This $\bar{a}$ value seems to be universal. From dominance of fluctuation for molecular glass transitions, we conclude that a reduction of $\dot{T}$ by δT (instead by T_g itself) is reasonable. Our $\bar{a}$ value means that a heating/cooling rate of 10 K/min corresponds to a frequency of 2 mHz for typical $\delta T = 3$ K values, and to 1 mHz for $\delta T = 6$ K.

Acknowledgements

The financial support from the Deutsche Forschungsgemeinschaft and from the Fonds der Chemischen Industrie is cordially acknowledged.

References

[1] N.O. Birge and S.R. Nagel, Phys. Rev. Lett., 54 (1985) 2674.
[2] B. Wunderlich, Thermal Analysis, Academic Press, Boston, 1990.
[3] G.B. McKenna, Comprehensive Polymer Science, Vol. 2, Polymer Properties, Pergamon, Oxford, 1990.
[4] Y.H. Jeong and I.K. Moon, Phys. Rev., B 52 (1995) 6381.
[5] D.H. Jung, T.W. Kwon, D.J. Bae, I.K. Moon and Y.H. Jeong, Meas. Sci. Technol., 3 (1992) 475.
[6] A. Hensel, J. Dobbertin, J.E.K. Schawe, A. Boller and C. Schick, J. Therm. Anal., 46 (1996) 935.
[7] M. Reading, Trends Polym. Sci., 1 (1993) 248.
[8] S. Weyer, A. Hensel, C. Schick, J. Korus, and E. Donth, this issue.
[9] J. Korus, Dissertation, Universität Halle, 1997.
[10] E. Donth, M. Beiner, S. Reissig, J. Korus, F. Garwe, S. Vieweg, S. Kahle, E. Hempel and K. Schröter, Macromolecules, 29 (1996) 6589.
[11] F. A. Garwe, A. Schönhals, H. Lockwenz, M. Beiner, K. Schröter and E. Donth, Macromolecules 29 (1996) 247; W. Domberger, D. Reichert, F. Garwe, H. Schneider and E. Donth, J. Phys.: Condens. Matter, 7 (1995) 7419.
[12] E. Donth, Relaxation and Thermodynamics in Polymers, Akademie Verlag, Berlin, 1992.
[13] L.D. Landau and E.M. Lifshits, Statistical Physics, Pergamon, Oxford, 1980.
[14] E. Donth, Glasübergang, Akademie-Verlag, Berlin, 1981.
[15] G. Adam and J.H. Gibbs, J. Chem. Phys., 43 (1965) 139.
[16] E. Donth, J. Non-Cryst. Solids, 53 (1982) 325.
[17] E. Donth, J. Polym. Sci. Polym. Phys. Ed., 34 (1996) 2887.
[18] O.S. Narayanaswamy, J. Amer. Ceram. Soc., 54 (1971) 491; M.A. De Bolt, A.J. Easteal, P.B. Macedo and C.T. Moynihan, J. Amer. Ceram. Soc., 59 (1976) 16; I.M. Hodge, Macromolecules, 20 (1987) 2897.
[19] J. Korus, M. Beiner, K. Busse, S. Kahle and E. Donth, this issue.
[20] M. Beiner, J. Korus, H. Lockwenz, K. Schröter and E. Donth, Macromolecules, 29 (1996) 5183.
[21] K. Schneider, A. Schönhals and E. Donth, Acta Polymer., 32 (1981) 471.
[22] Y.H. Jeong, this issue; N.O. Birge and S, R. Nagel, Phys. Rev. Lett., 54 (1985) 2674.
[23] K. Schneider, Dissertation, TH Merseburg, 1984 .
[24] B.W. Gnedenko, Lehrbuch der Wahrscheinlichkeitsrechnung. 8. Auflage, Harry Deutsch, Thun and Frankfurt A. M., 1987.
[25] S. Havriliak and S. Negani, J. Polym. Sci., C14 (1966) 99.